# Monitoring and structural significance of ground deformations at Campi Flegrei supervolcano (Italy) from the combined 2D and 3D analysis of PS-InSAR, geophysical, geological and structural data

G. Ventura*[a], Vilardo G. [b], V. Sepe[a]
[a] Istituto Nazionale di Geofisica e Vulcanologia, Via di Vigna Murata 605, Roma, Italy, 00143;
[b]Osservatorio Vesuviano- Istituto Nazionale di Geofisica e Vulcanologia, Via Diocleziano 328, Napoli, Italy, 80124

## ABSTRACT

Cities are growing around active volcanoes. Campi Flegrei supervolcano (CF, Italy) is a nested structure formed during two main collapses associated with two caldera-forming eruptions at 39 ka and 15 ka. The last event occurred in AD 1538 (Monte Nuovo volcano). CF hosts 350,000 people and two main uplift phases were recorded in 1968–1972 and 1982–1984 with deformations of about 2 m. The town of Pozzuoli was partially evacuated during the last crisis. Subsequent minor deformations (subsidence and uplift), seismicity, and diffuse $CO_2$ degassing concentrate in the central part of the caldera. Here, we apply the Permanent Scatterers Synthetic Aperture Radar Interferometry (PS-InSAR) to investigate the ground deformations of CF by using data acquired from 1993 to 2007 from ascending and descending tracks by ERS-1 ,ERS-2 and RADARSAT satellites. Deformation maps identify a subsidence interrupted by micro-uplift episodes. These maps are combined with digitized topographic, geological (faults and landslides), seismic, and urbanization data. The merged information allow us to identify the areas involved in the deformation and the volcano-tectonic structures activated during the uplift and subsidence episodes. We propose a structural-volcanological model for the unrest episodes. Data indicate that uplift episodes, which are associated to seismicity, are followed by subsidence episodes accommodated by pre-existing faults. The urbanized areas subjected to the higher deformations and shaking are also identified and mapped. A multi-hazard zonation including landslides is also provided. The approach used here may be utilized to (a) recognize the tectonic and/or volcanic structures activated during ground deformations, (b) to investigate structural models, (c) to evaluate and map multi-risk zonations, and (c) monitor other volcanic areas or non-volcanic zones subjected to gravity instability or tectonics.

**Keywords:** PS-InSAR, deformation, volcanology, tectonics, seismicity, risk zonation

## 1. INTRODUCTION

Remote sensing data by SAR interferometry (InSAR) have been used to detect and monitor ground deformations induced by landslides, volcanism, tectonics and anthropic processes in urbanized areas [1,2,3,4]. SAR imagery has been also utilized to analyze glacial features [5], climate changes [6], and land resources [7]. InSAR provides a one-dimensional measurement of change in distance along the look direction of the radar spacecraft (Line Of Sight, LOS). Recent advances in radar satellite capabilities (e.g., high spatial resolution and temporal frequency acquisitions) and the development of new techniques based on the interferometric analysis of large datasets such as the Permanent Scatterers (PS) technique [8], the Small Baseline (SBAS) [9] and Differential SAR Interferometry approach (DInSAR), have significantly increased the potential of SAR remote sensing. Here, we apply the Permanent Scatterers Synthetic Aperture Radar Interferometry (PS-InSAR) to investigate the ground deformations of the active Campi Flegrei supervolcano (CF; Southern Italy). The processing technique [8] bases on the identification of Permanent Scatterers (PS), which are man-made objects (statues, heating and ventilating structures on the roofs of buildings, utility poles, dams, etc.) or natural (rock outcrops) reflectors.

---

* Corresponding Author: G. Ventura; guido.ventura@ingv.it; phone +39 06-51860221; fax +39 06-5041303.

The phase data from PS are used to detect topographic changes by separating time-dependent surface motions, atmospheric delays, and elevation-error components of the range-change measurement. This technique has proved to be a powerful tool for exploring the slow movement of the earth's surface at local [10] and at sub-regional scale [11,12,13]. Our study on the CF area covers the June 1992-December 1999 time time interval and SAR data acquired from both ascending and descending tracks by ERS-1 and ERS-2 satellites. Data from ascending and descending tracks by RADARSAT satellite collected between October 2005 and November 2006 were also analyzed. The availability of ascending and descending datasets allow us to discriminate the vertical and east–west displacement components. The large spatial scale features of the investigated area, in which volcanic, tectonic, exogenous and anthropic processes coexist, are examined and digitally merged to the available geological and geophysical data. This information allow us to identify the areas involved in the deformation and the volcano-tectonic structures activated during uplift and/or subsidence episodes. We propose a structural-volcanological model for the unrest episodes. Data indicate that uplift episodes, which are associated to seismicity, are followed by aseismic subsidence episodes accommodated by pre-existing faults. The urbanized areas subjected to the higher deformations and shaking are also identified and mapped. A multi-hazard zonation is provided. The approach used here may be utilized to identify the active tectonic and/or volcanic structures and to monitor other volcanic or non-volcanic zones subjected to gravity instability phenomena and seismicity. To our knowledge, studies jointly discussing these processes in a single area are still lacking in literature.

## 2. GEOLOGICAL SETTING

CF caldera is an active volcanic field listed among the supervolcanoes of the world [14]. The caldera structure was mainly defined after the Campanian Ignimbrite supereruption (40 ka) and the Neapolitan Yellow Tuff eruption (15 ka). Both this large eruptions were accompanied by caldera collapse whose boundary are partly exposed on land, submerged or inferred by geophysical data (Fig. 1).The structural pattern of the caldera is dominated by NW-SE and NE-SW and subordinate N-S trending faults. A part of these major tectonic structures were reactivated through time inside the caldera and acted also as eruptive fissures for the volcanism younger than 15 ka. This volcanism was very intense with about 70 eruptions in three distinct epochs of activity alternating to long rest periods up to the last eruption of Monte Nuovo (1538 AD). Within the central-eastern sector of the caldera, at least for the last 9 ka, high frequency eruptions occurred in short time span and were characterized by different magnitude ranging from plinian to strombolian explosions and lava dome forming eruptions. Eruptions of the western sector were less frequent, and characterized by low energy explosive events. The Campi Flegrei caldera floor suffered repeated episodes of ground deformations more pronounced in the central sector where about 100 m of uplift were estimated in the last 10 ka. Before the eruptive activity, the central sector of the caldera was uplifted of few tens of meters following a magmatic chamber refilling.

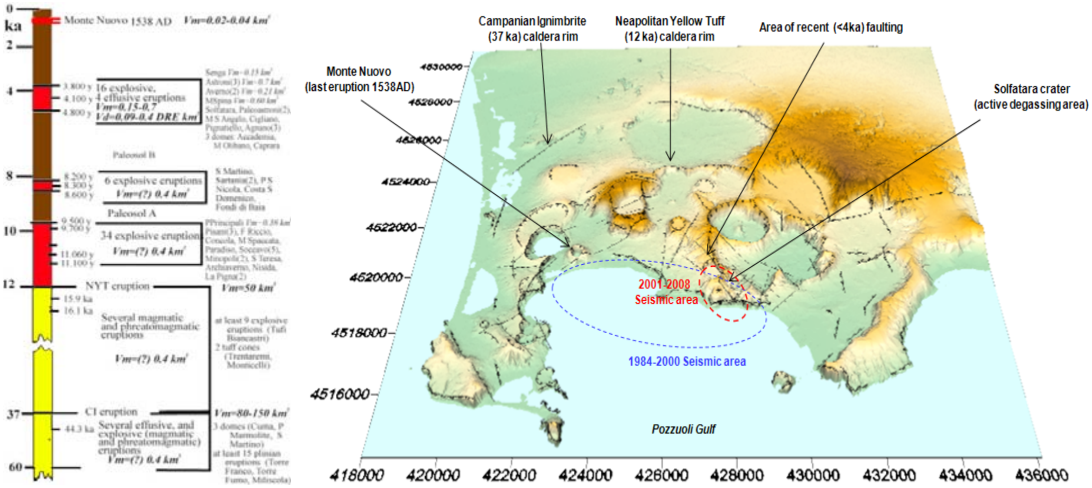

Fig. 1 Eruptive history and structural map of Campi Flegrei supervolcano

The still ongoing ground movement events (uplifts) periodically occurred during the last 2000 years without leading to eruptive activity. Two significant unrest crises leading also to a partial evacuation of the Pozzuoli town occurred on 1970-72 and 1982-84. During these crises a total ground uplift of 3.5 m were accompanied by thousands earthquakes, while only part of the displacement (less than 1 m) were recovered throughout the subsequent ground subsidence without seismicity. After the larger 1982-84 crises the general subsidence trend was interrupted by minor episodes of uplift and seismicity (few cm) with the last occurred in 2004-06. At the present, diffuse $CO_2$ degassing, seismicity, ground deformation, faulting and landslide occur in an area where 350,000 inhabitants occur.

## 3. CONSTRAINTS FROM SAR AND GPS DATA ON THE RATE AND SPATIAL PATTERN OF GROUND DEFORMATION

We use interferometric synthetic aperture radar (InSAR) permanent scatterer (PS) data to quantify the spatial pattern of the vertical and east–west components of the average surface deformation velocity for two distinct uplift and subsidence episodes. The average ground deformation velocity pattern associated to the last phase of subsidence lasting since 1985 was derived by applying the PSInSAR analysis (Ferretti et al., 2000, 2001) to a data set of SAR images acquired in the time interval June 1992 – December 1999 from both ascending and descending tracks by ERS-1 and ERS-2 satellites [4]. Whereas, the PSInSAR method applied to a temporal series of SAR scene acquired during the October 2005 – November 2006 time interval from both ascending and descending tracks by RADARSAT-1 satellite provided the overall picture of the ground deformation velocity for the last uplift phase started in the second half of 2004. The PS average displacement rates, in the line of sight (LOS) of the radar beam, obtained from the PSInSAR analyses were used to construct mean deformation velocity maps in SAR coordinates for both the ascending and descending orbits of the two distinct temporal series of SAR images. The availability of both ascending and descending datasets allowed us to separate, for the two analyzed deformation phases, the vertical and east–west components of the deformation by properly combining the radar LOS mean displacement velocity maps computed from the two SAR viewing geometries [4,15]. The maximum vertical surface velocity we compute for the subsidence phase (-34 mm/yr) is in full agreement with the value of -33 mm/yr obtained from high precision levelling data. For the uplift episode a maximum vertical ground velocity of 25 mm/yr was evaluated. The East-West displacements velocity patterns associated, respectively, to the subsidence episode (1992–1999) and to the subsequent uplift phase (2004–2005), show opposite trends as well. A summary of the velocity field is reported in Fig. 2.

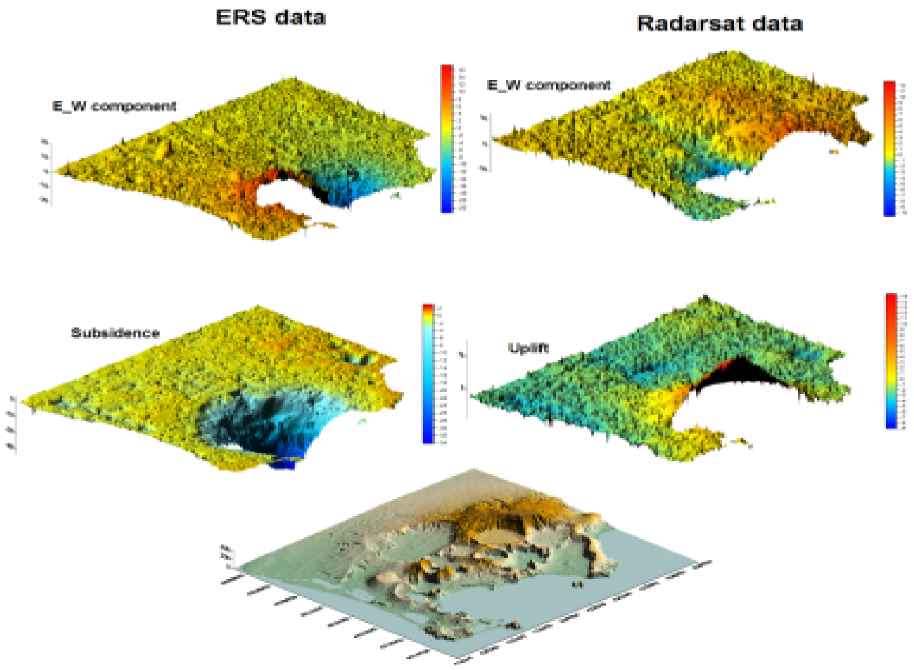

Fig. 2 Velocity fields deduced from the analysis of ERS and Radarsat data at CF supervolcano.

## 4. INTEGRATION OF SATELLITE, GEOLOGICAL AND GEOPHISICAL DATA: MULTIHAZARD ZONATION MAPS AND IDENTIFICATION OF THE ACTIVE STRUCTURES

The velocity pattern obtained from the analysis of satellite data have been integrated with other geological and geophysical data. These include, seismicity, landslides, faults, results from seismic lines. This integration allow us to visualize in a single frame the different types of hazard occurring during the uplift and/or subsidence episodes. Seismicity is associated to the uplift episodes and may induce fault re-activation on the surface and landslides. Fault-re activation and landslides may also occur without seismic activity during subsidence. Combined analysis of geological/deformation data allow us to identify the faults activated during the uplift or subsidence episodes (Fig. 3).

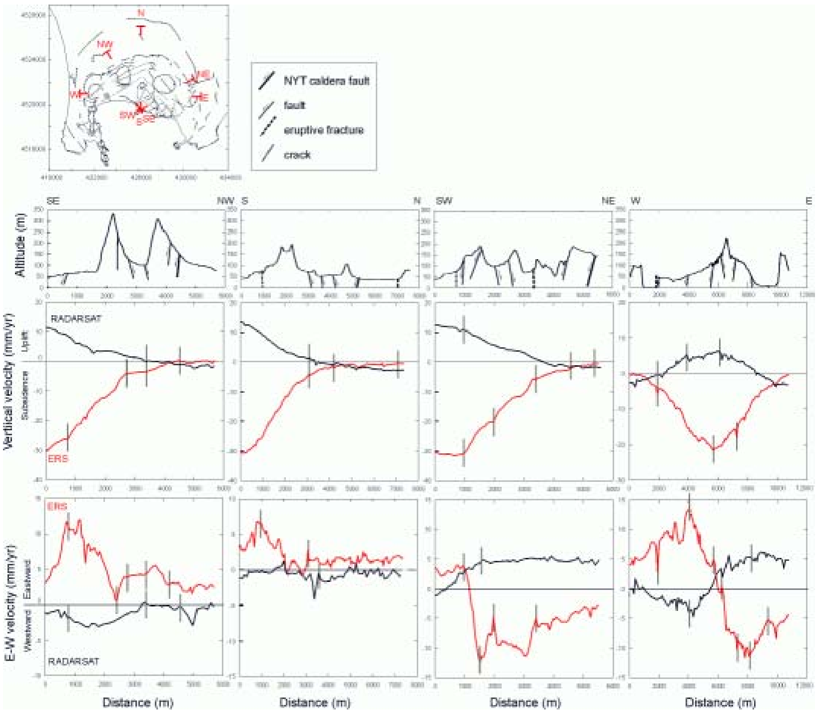

Fig. 3 velocity profiles along four different oriented sections within the CF supervolcano. The main faults, eruptive fractures, cracks and caldera rims are also reported. The vertical lines identify discontinuities in the velocity patterns spatially related to tectonic and volcano-tectonic structures.

The identification of such structures, combined on the spatial distribution of landslides allow us to propose a multi-risk zonation of the urban areas of the CF supervolcano (Fig. 4). Such zonation bases on the conceptual model of superimposed hazard for volcanic/tectonic areas, where a single endogenous process may trigger other (exogenous) phenomena. A particular type of risk is related to building crossed by faults that can activate with differential movements during horizontal deformations, so potentially triggering fault-induced landslides. Therefore, a map of the building crossed by faults covered by slides has been also produced

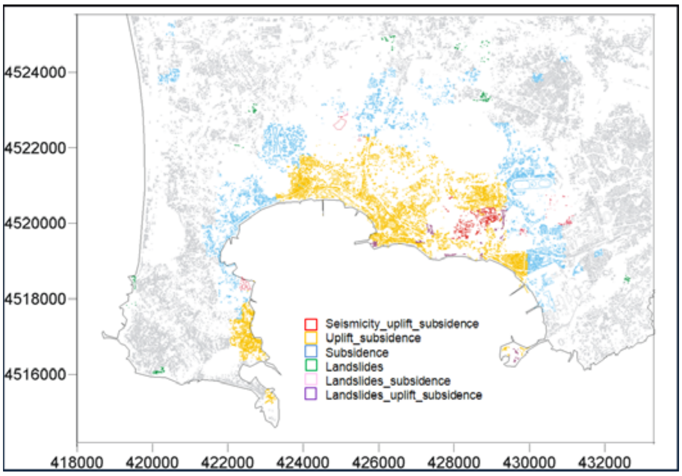

Fig. 4. Multi-risk zonation of the CF supervolcano suring quiescent stages relating uplift, subsidence, seismicity and sliding.

## 5. STRUCTURAL MODEL OF THE CAMPI FLEGREI SUPERVOLCANO

The combination of the structural, deformation and lines from seismic profiles allow us to propose a structural model for the CF caldera (Figs. 6, 7 and 8). Deformation phases are confined within the NYT caldera ring faults, which act as major discontinuities. NW-SE and NE-SW striking faults within the caldera are activated during the main uplift and subsidence episodes. A major N-S discontinuity opens during the uplift episodes producing local extension and closes during subsidence inducing local compression (Fig. 6). This discontinuity divides the CF caldera in two sectors and is located where the maximum uplift (or subsidence) velocity is detected. Seismic lines well evidence such discontinuity, which is defined by a set of N-S trending faults (Fig. 7).

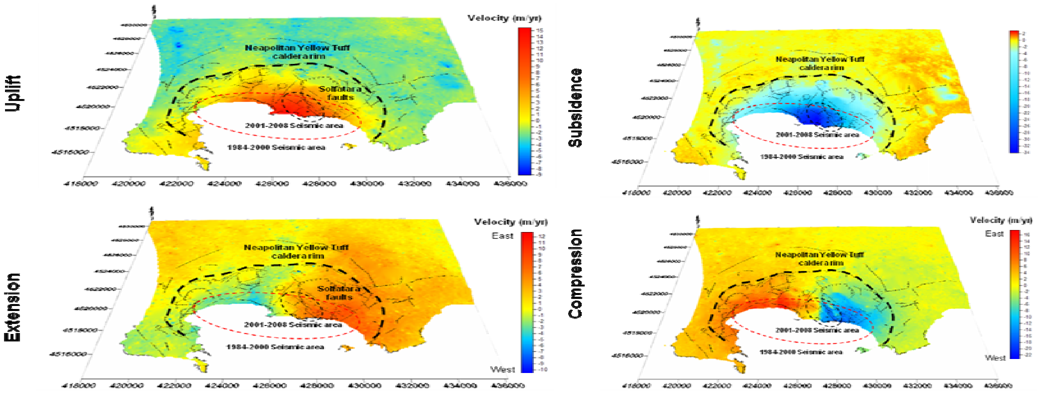

Fig. 6 Superimosed velocity fields, topography and structural pattern at CF caldera.

The uplift episodes are associated to seismicity. The envelope of hypocenters evidence the occurrence of a dome-like deformation field at 2-4 km depth, probably representing the top of a fluid-rich pocket uprising to the surface (Fig. 8).

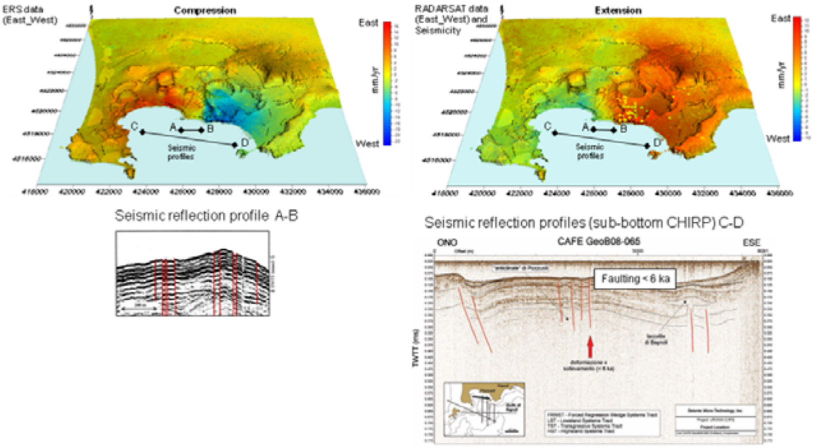

Fig. 7. Seismic lines evidence the caldera boundary faults and a set of N-S faults in the central sector of CF.

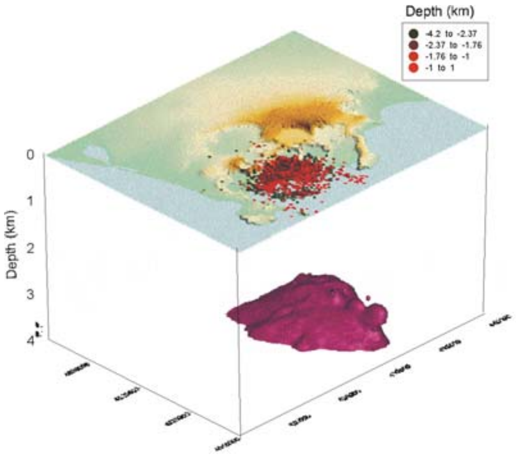

Fig. 8. Envelope of maximum depth of hypocenters of earthqaukes.

## 6. CONCLUSIONS

The results of this study may summarized in the following main points:

1) A multidisciplinary approach based on SAR-derived and geological-geophysical data is proposed to analyze changes in active volcanic and tectonic areas and evaluate the different risk factors. A case study from the densely inhabited (350,000 people) CF supervolcano is analyzed.
2) The multi-source data analysis allow us to propose a structural model of the observed deformation (velocity) field at CF. This permits to evaluate the cause-effect relationships maong different processes and to identify the major discontinuities governing the deformation field.
3) Fluids upraise from a dome-like hydrothermal system along identified faults and fractures during uplift at CF. Seismicity occurs only during the uplift phases due to a pore pressure increase. Aseismic creep characterizes subsidence (pore pressure decreases). The pre-existing caldera rims bound the zone affected by deformations (boundary effect).
4) The following risk factors are recognized during the quiescent activity in the densely populated area of CF: subsidence, uplift, horizontal deformation, faulting, landslides, seismicity and some combinations among these processes.

5) A zonation of urban areas based on the different risk factors or a combination of factors is proposed based on the analysis of digital multi-source data

The approach presented here may be extended to other active volcanic, hydrothermal and/or tectonic (seismic) areas.

## REFERENCES

[1] Achache, J., B., Fruneau, and Delacourt, C. "Applicability of SAR interferometry for operational monitoring of landslides. " Proceedings of the Second ERS Applications Workshop, London, 165−168 (1995).

[2] Kimura, H., and Yamaguchi, Y. "Detection of landslide areas using radarinterferometry. " Photogrammetry Engineering and Remote Sensing, Vol. 66, 337−344 (2000).

[3] Tizzani, P., P., Berardino, F., Casu, P., Euillades, M., Manzo, Ricciardi, G. P. "Surface deformation of Long Valley caldera and Mono Basin, California, investigated with the SBAS-InSAR approach 2007. " Remote Sensing of Environment, Vol. 108, 277−289 (2007).

[4] Vilardo, G., G., Ventura, C., Terranova, F., Matano, and Nardò, S. "Ground deformation due to tectonic, hydrothermal, gravity, hydrogeological, and anthropic processes in the Campania Region (Southern Italy) from Permanent Scatterers Synthetic Aperture Radar Interferometry. " Remote Sensing of Environment doi:10.1016/j.rse.2008.09.007 (2009)

[5] Mark, B., G., Seltzer, and Geoffrey, O. "Evaluation of recent glacier recession in theCordillera Blanca, Peru (AD 1962–1999): spatial distribution of mass loss and climatic forcing. " Quaternary Science Reviews, Vol. 24, 2265−2280 (2005).

[6] Beer, J., W., Mende, and Stellmacher, R. "The role of the sun in climate forcing. " Quaternary Science Reviews, Vol. 19, 403−415 (2000).

[7] Legesse, D., and Ayenew, T. "Effect of improper water and land resource utilization on the central Main Ethiopian Rift lakes. " Quaternary International, Vol. 148, 8−18 (2006).

[8] Ferretti, A., C., Prati, and Rocca, F. "Nonlinear subsidence rate estimation using Permanent Scatterers in differential SAR interferometry. " IEEE Transactions on Geoscience and Remote Sensing, Vol. 38, 2202−2212 (2000).

[9] Berardino, P., G., Fornaro, R., Lanari, and Sansosti, E. "A new algorithm for surface deformation monitoring based on small baseline differential SAR interferograms. " IEEE Transactions on Geosciences and Remote Sensing, Vol. 40, 2375−2383 (2002).

[10] Hilley, G. E., R., Bűrgmann, Ferretti, A., F., Novali, and Rocca, F. "Dynamics of slowmoving landslides from permanent scatterer analysis. " Science, Vol. 304, 1952−1955 (2004).

[11] Bűrgmann, R., G., Hilley, A., Ferretti, and Novali, F. "Resolving vertical tectonics in the San Francisco Bay Area from permanent scatterer InSAR and GPS analysis. " Geology, Vol. 34, 221−224 (2006).

[12] Farina, S., D., Colombo, A., Fumagalli, F., Marks, andMoretti, S. "Permanent Scatterers for landslide investigations: outcomes from the ESA-SLAM project. " Engineering Geology, Vol. 88, 200−217 (2006).

[13] Meisina, C., F., Zucca, D., Fossati, M., Ceriani, and Allievi, J. "Ground deformation monitoring by using the Permanent Scatterers Technique: the example of the Oltrepo Pavese (Lombardia, Italy) ". Engineering Geology, Vol. 88, 240−259 (2006).

[14] Miller, C.F., and Wark D.A. "Supervolcanoes and their supereruptions." Elements, Vol. 4, 11-16 (2008)

[15] Manzo, M., G. P., Ricciardi, F. Casu, Ventura, G., Zeni, G., and Borgström, S., "Surface deformation analysis in the Ischia Island (Italy) based on spaceborne radar interferometry." Journal of Volcanology and Geothermal Research, Vol. 151, 399−416 (2006).